Article

Rapid UV Photo-Cross-Linking of α-Lactalbumin Hydrogel Biomaterial To Enable Wound Healing

Yaqing Huang, Qinchao Zhu, Yang Zhu, Teresa G. Valencak, Ying Han, Tanchen Ren,* Chengchen Guo,* and Daxi Ren*

Read Online

ACCESS | Metrics & More | Article Recommendations

ABSTRACT: Although both the function and biocompatibility of protein-based biomaterials are better than those of synthetic materials, their usage as medical material is currently limited by their high costs, low yield, and low batch-to-batch reproducibility. In this article, we show how α-lactalbumin (α-LA), rich in tryptophan, was used to produce a novel type of naturally occurring, protein-based biomaterial suitable for wound dressing. To create a photo-cross-linkable polymer, α-LA was methacrylated at a 100-g batch scale with >95% conversion and 90% yield. α-LAMA was further processed using photo-cross-linking-based advanced processing techniques such as microfluidics and 3D printing to create injectable hydrogels, monodispersed microspheres, and patterned scaffolds. The obtained α-LAMA hydrogels show promising biocompatibility and degradability during in vivo testing. Additionally, the α-LAMA hydrogel can accelerate post-traumatic wound healing and promote new tissue regeneration. In conclusion, cheap and safe α-LAMA-based biomaterials could be produced, and they have a beneficial effect on wound healing. As a result, there may arise a potential partnership between the dairy industry and the development of pharmaceuticals.
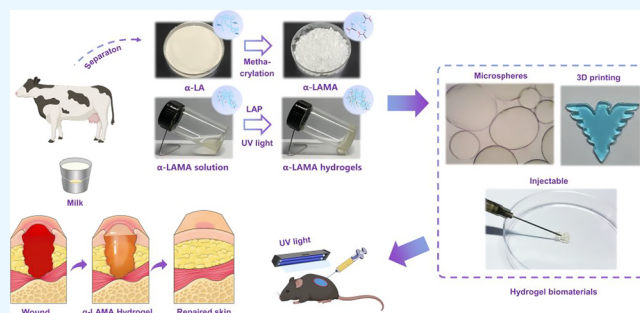
1. INTRODUCTION

Naturally occurring proteins, such as collagen and silk, are crucial to biological systems. They support the morphological and physiological characteristics of tissues and organs while regulating the behavior and development of cells. Compared with synthetic materials, biomaterials based on proteins have better biocompatibility and function. In recent years, the development of biomaterials based on natural proteins for therapeutic applications has emerged as a dynamic and appealing area of research.[1,2] However, harvesting and processing of natural proteins is associated with high costs and unstable properties.[2] Thus, the utilization of natural protein biomaterials as medical materials is rare compared to synthetic materials. Scaffolds and hydrogels produced from collagen, gelatin, silk, keratin, elastin, and fibrin make up the majority of natural protein biomaterials used for medical properties.[3,4]

Milk has a wide range of nutritional and medicinal benefits and provides a rich source of protein. α-Lactalbumin (α-LA) is a small (M_r 14.2 kDa), acidic (pI 4−5) globular protein found in the whey fraction of milk in all mammals.[5] α-LA is the second most abundant protein in bovine whey with a concentration of approximately 2.44 g/L in milk.[6] Bovine and human α-LA show 74% sequence identity, similar bioactivities, and similar amino acid contents.[7] Additionally,

it is a rich source of tryptophan, a building block needed to synthesize the neurotransmitter serotonin.[7] According to recent studies, serotonin can accelerate keratinocyte and fibroblast migration and proliferation, promoting skin wound healing in burn patients.[8,9] α-LA preparations show good protein quality, high water solubility across a broad pH range (2.0−9.0), and high heat stability, making them optimal for the creation of gels, foams, and emulsions.[10,11] α-LA, on the other hand, has numerous advantageous qualities that make it a feasible biomaterial with low immunogenicity, minimal risk of disease transmission, and bioactivities relating to an antitumor, antibacterial, antioxidant, and antihypertensive effect.[12,13]

In recent years, a-LA research has become more intensive in the medical field. Xiong et al. developed an a-lactalbumin-based nanofiber dressing to improve burn wound healing and reduce scarring.[14] Liu et al. designed α-LA self-assembled nanoparticles as Pickering stabilizers for curcumin delivery.[15]
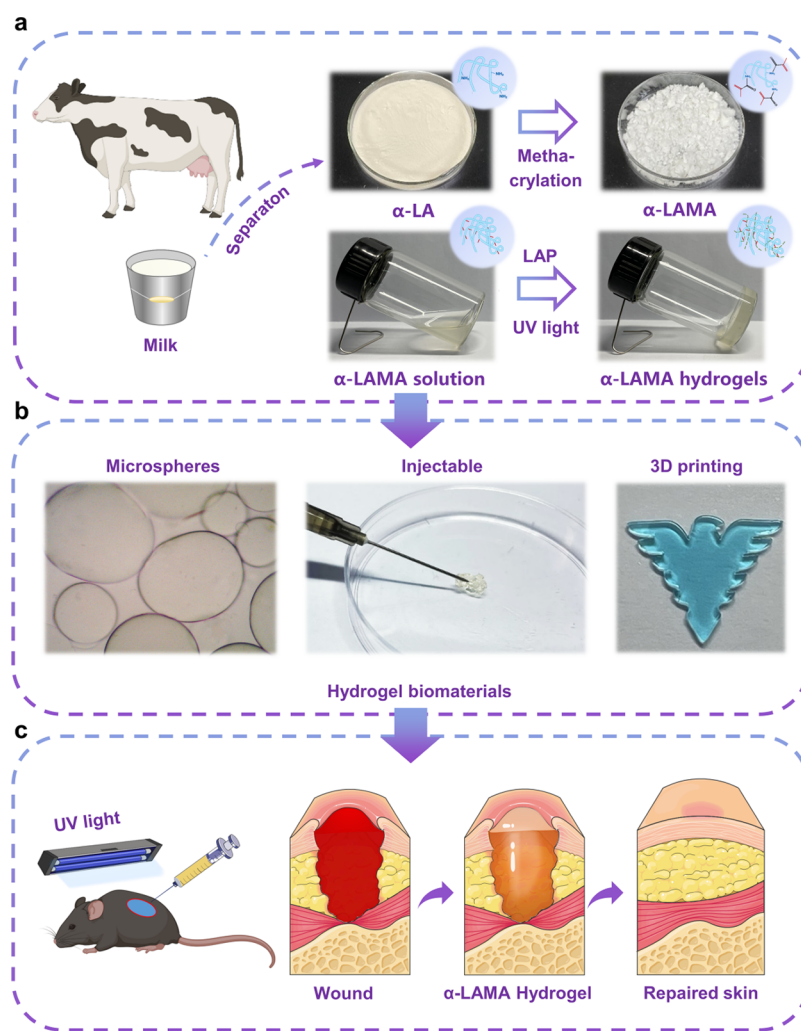
Figure 1. Schematic illustration of the preparation of α-LAMA hydrogels. (a) α-LA was methacrylated into α-LAMA and then cross-linked through UV light formation initiated by LAP to form the hydrogel. (b) α-LAMA was processed into injectable hydrogels, monodispersed microspheres, and patterned scaffolds. (c) Process of wound healing after treatment with α-LAMA hydrogel.

However, there are few studies out there that support the use of α-LA hydrogels as a medical material.

Here, we created a hydrogel based on α-LA as a practical treatment in wound healing. We methacrylated α-LAs and created bulk hydrogels by photo-cross-linking the modified α-LAs (α-LAMA) (Figure 1a). The investigation delved into the photo-cross-linking behavior of α-LAMA, scrutinizing the physical characteristics of the resulting α-LAMA hydrogels. This comprehensive analysis aimed to discern the ideal methacrylation ratio and protein concentration that would yield optimal properties for the hydrogels. Monodispersed microspheres and patterned hydrogel structures were fabricated, showcasing the photo-cross-linkable nature of α-LAMA that aligns using precision manufacturing techniques, such as microfluidics and digital light-processed 3D printing (Figure 1b). The degradability and biocompatibility of the new α-LAMA hydrogels were tested in mice through subcutaneous implantation and hemocompatibility. Finally, the α-LAMA hydrogel dressing was created at the wound site through covalent cross-linking under UV light to assess its wound healing property (Figure 1c). Our results suggest that α-LA-based medical materials have a significant potential for being clinically translated and widely used for biomedical applications.

2. MATERIALS AND METHODS

2.1. Preparation of Methacrylated α-LA Powder. α-LAs were purchased from Tianjin Milkyway Import & Export Co. A quantity of 1 g of α-LAs was dissolved in 9 mL of 1× phosphate-buffered saline (PBS) at room temperature. Next, 0.025, 0.05, or 0.1 mL of methacrylic anhydride (purity 94%, with 0.2% topanol) (Macklin Biochemical Co., Ltd., Shanghai, China) was added to the α-LA solution. Then, 5 M NaOH solution was then used to adjust the pH to 8.0. Finally, PBS was used to fill up the volume to 10 mL. Finally, methacrylated (α-LAMA) solutions were freeze-dried for 24 h before being frozen at 80 °C for 12 h. For later use, lyophilized α-LAMA powder was conserved at 80 °C.

2.2. Methacrylation Degree of α-LAMA. The methacrylation degree of α-LAMA was determined through formaldehyde titration. 0.2 g of the sample was dissolved in 150 mL of deionized water at 40 °C and then allowed to cool down to room temperature. 0.02 mol/L NaOH solution was added dropwise until the pH of the sample solution was 9, and then 25 mL of formaldehyde solution (10%) was added to the mixture. Next 0.02 mol/L NaOH solution was used to stabilize the pH of the sample solution back to 9. Deionized water was used as a blank control. The aforementioned operation was

repeated, and by deducting the volume of NaOH solution, the molar amount of NaOH consumed was defined as the sample amino content.

The methacrylation degree of α-LAMA was calculated as follows:

$$\text{Methacrylation degree}(\%) = \frac{A(\alpha - \text{LAMA})}{A(\alpha - \text{LA})} \times 100\%$$

$A(\alpha\text{-LAMA})$ represents the amino group content (mol/g) of the α-LAMA sample, and $A(\alpha\text{-LA})$ denotes the average amino group content (mol/g) of α-LAs.

2.3. Nuclear Magnetic Resonance Spectroscopy. NMR spectra were obtained using a Bruker AVANCE NEO 600 MHz NMR spectrometer equipped with a cryo-probe. The samples were dissolved in an H_2O/D_2O mixture (90/10, v/v) to achieve a concentration of 6 wt % for NMR characterization. Heteronuclear single quantum coherence (HSQC) spectra for 1H-13C were recorded with a 180 ppm spectral width in the $t1$ dimension and an 18 ppm spectral width in the $t2$ dimension. Acquisition parameters included 256 complex points in the $t1$ dimension, 2048 complex points in the $t2$ dimension, and 16 scans.

2.4. Circular Dichroism Spectroscopy. CD spectra were acquired by utilizing a Chirascan V100 instrument (Applied Photophysics, England) within the wavelength range of 180–260 nm. The samples were dissolved at a concentration of 0.1 mg/mL in deionized (DI) water. Each measurement consisted of three readings, and the background spectrum was obtained using DI water. The final spectrum was derived from the average of the three measurements.

2.5. Rheology. The rheological properties, including the dynamic storage modulus (G') and loss modulus (G''), of α-LA were assessed by using a rheometer (MCR302, Anton Paar, Austria) equipped with a Peltier element for precise temperature control and a UV generator. For each experimental condition, freeze-dried α-LAMA powder was prepared at concentrations of 15, 20, 25, or 30% (w/v) with varying methacrylation degrees (24, 57, or 99%). Dissolving the powder in distilled water, a photoinitiator, LAP (0.05% w/v, Tokyo Chemical Industry, Tokyo, Japan), was meticulously added and thoroughly combined until complete dissolution was achieved. The resulting α-LAMA solutions were carefully positioned between the rheometer plates at 37 °C, ensuring complete gap filling (1 mm). Oscillatory time sweep measurements were performed under 365 nm UV irradiation with an intensity of 12 mW/cm^2. The experiments were conducted at a frequency of 50 Hz and a strain of 1%.

2.6. Scalable Production of α-LAMA. A 100 g unit of α-lactalbumin (α-LA) was meticulously dissolved in 900 mL of PBS at room temperature. Subsequently, 20 mL of methacrylic anhydride (Macklin Biochemical Co., Ltd., Shanghai, China) was introduced into the α-LA solution. The pH of the solution was meticulously adjusted to 8 by adding 5 M NaOH, and then PBS was used to make the final volume reach 1 L. Stirring at 200 rpm was continued for 24 h at 25 °C, maintaining the pH at 8.0 throughout the process.

The resulting solution underwent a 5-fold dilution with distilled water and was subjected to ultrafiltration at 25 °C using an HMTECH-UF1812 benchtop ultrafiltration system (Huamo Technology Co. Ltd., Hangzhou, China). The ultrafiltration process was carried out using a poly(ether sulfone) (PES) membrane with a molecular weight cutoff

(MWCO) of 5 kDa, and the transmembrane pressure was set at 0.85 MPa. The solution underwent concentration during each ultrafiltration round, with a total of five five-fold concentration cycles. Following each run, distilled water was introduced to replenish the feed solution to its initial volume of 1 L.

The final concentrated solution underwent freeze-drying for 24 h after being prefrozen at −80 °C for 12 h. This method ensured the purification and concentration of methacrylated α-LA for subsequent experimental applications.

2.7. Preparation of α-LAMA Hydrogels. The freeze-dried α-LA powder was dissolved in a LAP solution with a concentration of 0.05% w/v at varying concentrations, including 15% w/v, 20% w/v, 25% w/v, or 30% w/v. Subsequently, these solutions underwent exposure to UV light with a wavelength of 365 nm and a power level set at 30 mW cm^{-2}.

2.8. Mechanical Characteristics. A compression experiment was conducted using mechanical testing equipment (5543A, Instron, USA) to ascertain the compressive modulus of the α-LAMA hydrogel at various concentrations (15% w/v, 20% w/v, 25% w/v, or 30% w/v) and a methacrylation degree of 99%. The hydrogels were synthesized using the same procedure as given in section 2.7, but in 2 mL syringes, and they were then pressed into cylindrical shapes for the compression test. The compressive modulus for each sample was assessed by analyzing the slope within the elastic range (10–20% strain) in the stress−strain curves at a 5 mm/min compression speed. An average value for each group was calculated from five measurements.

2.9. Swelling Test. The initial weights of α-LAMA hydrogels (15% w/v, 20% w/v, 25% w/v, or 30% w/v) with a diameter of 8 mm and height of 6 mm and a 99% methacrylation degree were accurately measured upon fabrication. Subsequently, these hydrogel samples were immersed in 15 mL of PBS (pH 7.4) buffer at room temperature until they reached an equilibrium state. The enlarged hydrogels were then gently drained of excess water using filter paper, and they were weighed at scheduled intervals. Average values for each group were derived from five samples.

The swelling ratio of the α-LAMA hydrogels was defined as follows:

$$\text{Swelling ratio}(\%) = \frac{M_i - M_0}{M_0} \times 100\%$$

where M_i and M_0 refer to the weights of the swollen and initial samples, respectively.

2.10. Morphological Characterization. The examination was conducted by using inverted optical microscopy and field-emission scanning electron microscopy (SEM). (GeminiSEM 300, Carl Zeiss, Germany). Pore diameters of hydrogel samples were measured using ImageJ 1.53t. Three images of each hydrogel sample were shot from different angles (there were at least three samples per hydrogel). We used Origin 2023 to analyze the aforementioned data and perform a normal distribution analysis.

2.11. Preparation of α-LAMA Hydrogel Microspheres. To create α-LAMA microspheres, α-LAMA with a methacrylation degree of ≥99% was used. Paraffin oil and Span 80 comprised the continuous phase, while 20% w/v α-LAMA and LAP served as the initiators during the dispersed stage. The

flow rates for the dispersed stage were 100 μL h^{-1}, while the continuous phase was 6 mL h^{-1}. α-LAMA droplets were subjected to 365 nm UV exposure for 5 min at a maintained microfluidic channel. By centrifuging the cross-linked microspheres at 1000 rpm for 5 min, they were extracted. N-hexane and deionized water were used to clean the continuous phase.

2.12. Particle Size Statistics of α-LAMA Microspheres. α-LAMA hydrogel microspheres were appropriately diluted in PBS in a 50 mm Petri dish. A biologic microscope (CX31, Olympus, Japan) was used to obtain 20 photos at random. Using ImageJ 1.53t, the microsphere size distribution of the α-LAMA hydrogel was measured and examined.

2.13. Digital Light Processing 3D Printing. α-LAMA solution at a concentration of 20% (w/v) was used to conduct the test. The DLP printing system and 3D molds with the desired structures were designed, converted, and sliced, following the procedures outlined in our previous study.[16] A 20% (w/v) α-LAMA solution sample was deposited onto the print station. The printing parameters were configured as follows: printing thickness of 50 μm with an exposure time of 60 s. Following the printing process, the constructs were rinsed with PBS to eliminate any uncross-linked solution.

2.14. Characterization of Hemocompatibility. The hemolysis test aimed to assess the hemocompatibility of the hydrogel.[17,18] Human whole blood from a healthy donor was utilized for the experiment. Saline served as the negative control, while ultrapure water acted as the positive control. Initially, 1 mL solutions with varying mass concentrations (1, 3, 5, 7, and 10 mg/mL) of α-LAMA hydrogels were prepared in a saline solution for the sample group. Fresh blood was diluted with saline in an 8:10 ratio. Subsequently, 20 μL of the diluted blood was added to each group and incubated at 37 °C for 1 h. After incubation, 1 mL of saline containing different samples was collected, and the suspension underwent centrifugation at 1000 rpm for 10 min. The absorbance of the supernatant was measured at 545 nm by using an enzyme marker.

The hemolysis rate was defined as follows:

$$\text{Haemolysis rate}(\%) = \frac{\text{OD}_I - \text{OD}_N}{\text{OD}_P} \times 100\%$$

where OD_I, OD_N, and OD_P refer to the absorbances of the experimental group and the negative and positive control group, respectively.

2.15. Mice Subcutaneous Implantation. α-LAMA with a methacrylation degree ≥99% was applied to prepare an α-LAMA hydrogel to be used for subcutaneous implantation into mice. 20% w/v α-LAMA solution was subjected to UV light exposure to facilitate the formation of cylindrical hydrogels. Subsequently, The hydrogel was divided into 0.1 g portions. Male C$_{57}$BL/6 N mice aged 7 weeks were anesthetized with 1% pentobarbital (50 mg kg^{-1}). After removal and disinfection of the dorsal hair, the prepared α-LAMA hydrogel was implanted subcutaneously into the mice. On days 7, 28, and 84 postimplantation, the animals were euthanized, and a photo was taken to document the effects of the hydrogels on the surrounding tissue.

2.16. Inflammatory Cytokine Analysis In Vivo. First, the α-LAMA hydrogel was subcutaneously implanted into mice. Blood samples were collected from various groups of mice on days 1, 3, and 5, into 1 mL centrifuge tubes without additives. After allowing the blood samples to clot for 30 min

at 25 °C, they were centrifuged at 2000 rpm for 10 min at 4 °C. The resulting serum was obtained and stored at −80 °C until analysis. The analysis of all inflammatory cytokine markers was conducted using ELISA Kits.

2.17. Cytotoxicity of α-LAMA Hydrogel. The cytotoxicity of the hydrogel was assessed using a method that had been previously described.[19] The α-LAMA hydrogels with a methacrylation degree of ≥99% were used for testing. In short, 50 mg of bulk hydrogel was added per mL of DMEM, and then the hydrogel was immersed in DMEM at 37 °C for 24 h. Endothelial cells were cultured in 96-well plates with 200 μL of the resulting supernatant for 24 h. Fresh DMEM served as a control, and subsequently, the culture medium was replaced with 200 μL of fresh DMEM containing 20 μL of a CCK-8 solution. After a 2 h incubation, the absorbance of the medium at 450 nm was measured using a microplate reader (Tecan M200 PRO, Tecan, Switzerland).

2.18. In Vivo Wound Healing Performance of α-LAMA Hydrogel. For the wound-healing experiment, male C$_{57}$BL/6 N mice aged 7 weeks were chosen as subjects to assess the wound-healing effect of the α-LAMA hydrogel. All mice were split into three groups at random: the control group, the Gauze group, and the α-LAMA group. The control group received no medical attention, the Gauze group was covered with gauze, and the α-LAMA group was treated with the α-LAMA hydrogel.

Following anesthesia induced by intraperitoneal injection of 1% pentobarbital (50 mg kg^{-1}), the dorsal skin of all mice underwent shaving, and any remaining hair was fully removed using depilatory cream for 5 min. A fully circular wound of 7 mm diameter was generated in the center of each mouse's dorsal area. Subsequently, the α-LAMA hydrogel precursor solution was applied to fill the wounds and cross-linked in situ for 45 s using a 365 nm UV flashlight. Finally, the wound covered with the α-LAMA hydrogel was wrapped with sterile gauze. At predetermined time points, all mice were euthanized and the wound tissues were collected for histological examination. The dressings were changed every 3 days, and the wounded areas were photographed and evaluated using ImageJ 1.53t.

The wound closure in different groups was defined as follows:

$$\text{Wound closure}(\%) = \frac{S_i}{S_0} \times 100\%$$

where S_i means the remaining wound area at each time point and S_0 means the initial area of the wound.

2.19. Histopathological Study. The wound tissues were fixed in 4% paraformaldehyde, embedded in paraffin, and sectioned into 5 μm slides. Following deparaffinization, histological analysis was conducted with hematoxylin and eosin staining, and collagen quantification was performed using Masson staining (Solarbio, G1340, China). Microscopic images were captured using a Leica DM3000 microscope from Germany.

Histological wound samples were collected on days 7 and 10. All collected samples were fixed in a 4% paraformaldehyde solution and embedded in paraffin to prepare tissue slides with a thickness of 5 μm. Representative specimens were stained with hematoxylin and eosin (H&E) as well as Masson trichrome for histological observation using microscopy.
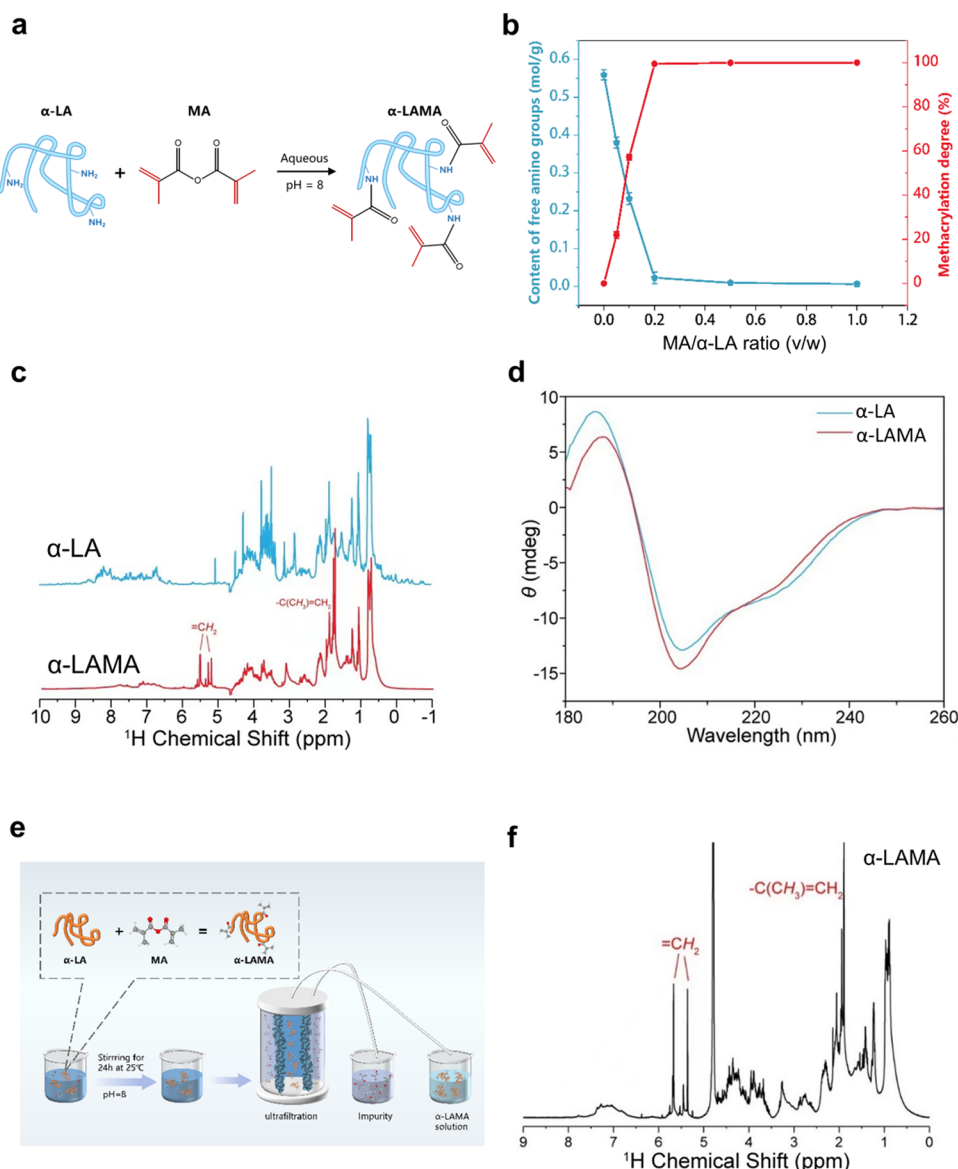
Figure 2. Production, characterization, and structure of α-LAMA. (a) α-LA undergoes methacrylation through the use of methacrylic anhydride (MA). (b) Free amino group content (blue circle) and methacrylation degree of α-LAMA (red circle) produced at different MA/α-LA ratios. (c) ^{1}H NMR spectra of α-LA and α-LAMA. (d) CD spectra of α-LA and α-LAMA. (e) Pilot-scale production of α-LA as prehydrogels. (f) ^{1}H NMR spectra of α-LAMA produced in pilot scale.

2.20. Statistics. All data are presented as means ± standard deviations (SD) from experiments conducted in triplicate or more. Statistical analysis was performed by using GraphPad Prism 7. Unpaired two-tailed Student's t-tests were conducted for comparisons between two groups, and one-way ANOVA was employed for more than two groups. Statistically significant differences are indicated with *$p < 0.05$, **$p < 0.01$, and ***$p < 0.001$.

3. RESULTS

3.1. Methacrylation of α-LA. Methacrylic anhydride (MA) is a potent and commonly employed electrophilic reagent for the substitution of methacrylate groups, which was previously used to react with primary amine in biopolymers. For this purpose, α-LAMA was created by adding MA to a solution of α-LA that had a pH of 8 (Figure 2a). Following purification by dialysis, the 1H NMR spectra revealed the characteristic peak resonances of the methacrylate vinyl group

(= 5.4 ppm) and the methyl group of α-LAMA (= 2.8 ppm). (Figure 2c). Following methacrylation, there was no discernible change in the proteins' secondary structure according to CD spectra (Figure 2d). The α-LAMA was synthesized by adding different concentrations of MA to an α-LA methacrylation solution to identify the best MA solution for efficient methacrylation. Formaldehyde titration was then used to determine the degree of methacrylation. Notably, once the MA to α-LA ratio arrived at 0.2 (v/w), almost all free amino groups in α-LA underwent chemical modification. The percentages of methacrylation on α-LA at 0.05 (v/w) and 0.1 (v/w) MA/α-LA concentration ratios were 24 and 57%, respectively (Figure 2b).

Thus, we concluded that the replacement of primary amines in α-LA with methacrylate groups is possible. Therefore, methacrylated α-LA can be used as a starting material for photopolymerization to create the hydrogel.
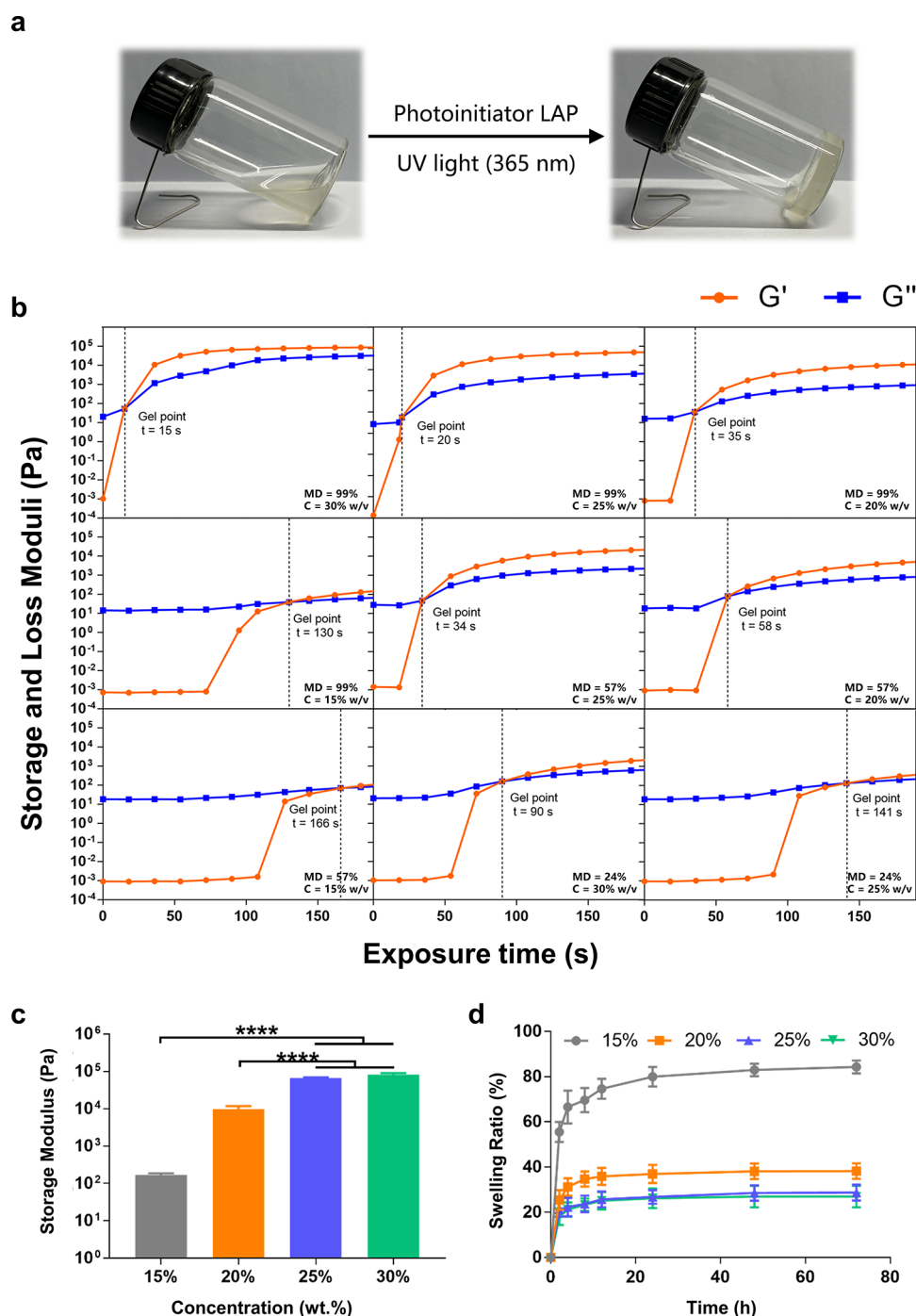
Figure 3. Photo-cross-linking, gelation dynamics, and characterization of α-LAMA hydrogels. (a) Picture of α-LAMA photo-cross-linking to form a hydrogel when LAP is present. (b) Rheological examination of the gelation of α-LAMA hydrogels (24, 57, and 99% of α-LAMA) methacrylated at different concentrations (15, 20, 25, and 30%) with UV (365 nm) irradiation. (c) Storage modulus of 99% of α-LAMA hydrogels was methacrylated at different concentrations (15, 20, 25, and 30%). (d) Swelling ratio with 99% of α-LAMA hydrogels (15, 20, 25, and 30%) at different time points. α-LAMA with $a \geq 99\%$ methacrylation (20% mass ratio of MA to α-LAs in the reaction) was used to prepare differently formed α-LAMA hydrogels.

3.2. Scalable Production of α-LAMA. To optimize α-LAMA production speed and scale, α-LAMA was chemically synthesized by modifying 100 g of α-LA with 20 mL of MA at pH 8 for 24 h (Figure 2e). The produced α-LAMA was then recovered by ultrafiltration and lyophilization. In less than 72 h, this production method yielded >90 g of α-LAMA per batch. The process also took less time than the small-scale α-LAMA manufacturing (10 g per batch), in which chemically modified

α-LA was first purified using dialysis before being lyophilized. The α-LAMA had a methacrylation degree of over 95%, which was equivalent to α-LAMA generated at a scale of 10 g.

For their use in medical implants and translational research, scalable production with consistent reproducibility and stringent quality control is crucial, but naturally derived, protein-based biomaterials are weak in this regard. The production is ecologically friendly when performed in a well-
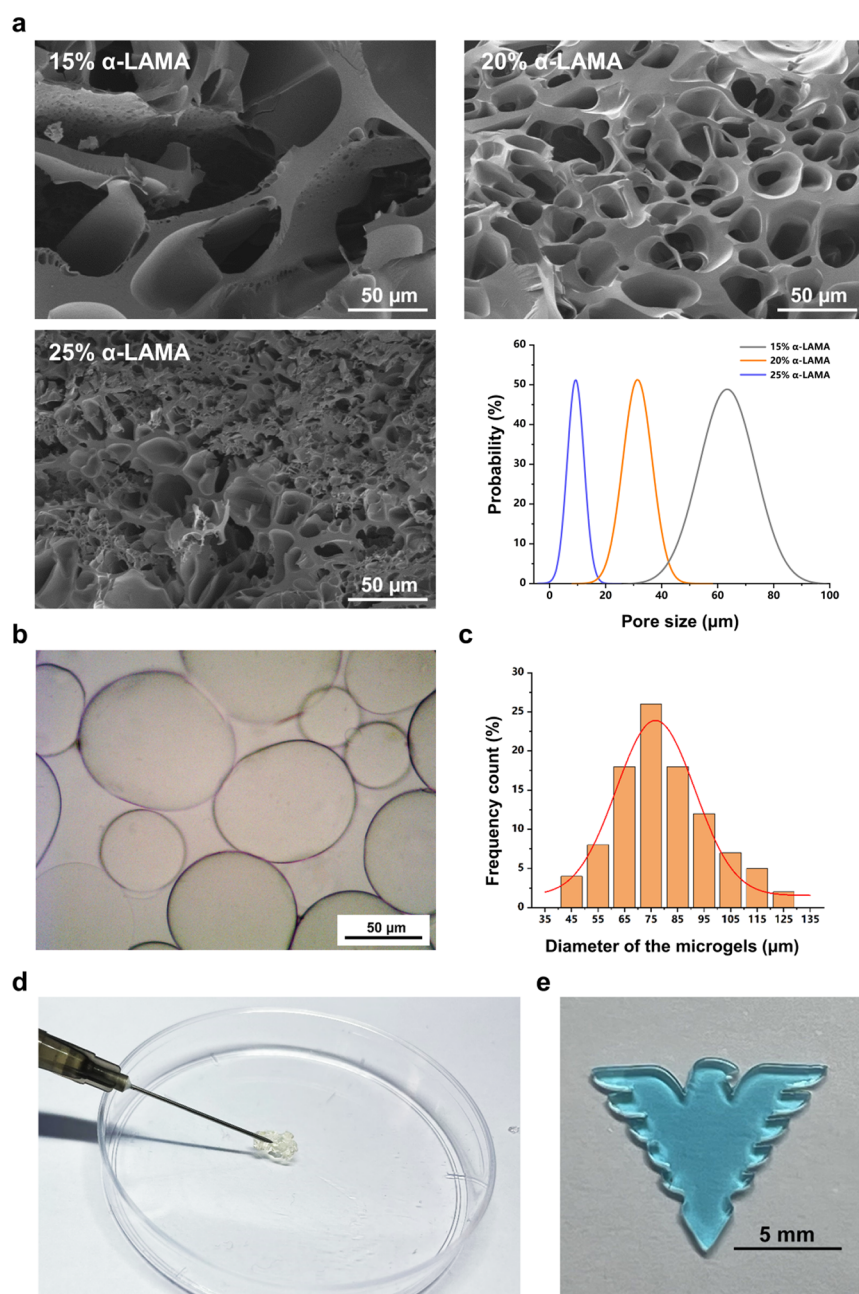
Figure 4. Variations in α-LAMA hydrogel forms. (a) Microstructure of freeze-dried α-LAMA hydrogels (15, 20, and 25%) observed under SEM and pore size distribution of different hydrogels. (b) Hydrogel microspheres produced using a microfluidic technology. (c) Particle size distribution for microspheres. (d) Hydrogel injected from a 26 G needle. (e) Eagle-patterned (i.e., logo of Zhejiang University) hydrogel 3D printed with the DLP device.

controlled manner. A straightforward and effective approach was used in our investigation to produce α-LAMA in large amounts up to 100 g, demonstrating that it has realistic potential for future applications. Altogether, the adverse effects of α-LAMA production are minimal and the production might be scaled up to the industrial level.

3.3. Preparation and Characteristics of α-LAMA Hydrogels. The rheological characteristics of α-LAMA were continuously monitored throughout the UV-curing reaction (during which UV light "dries" the hydrogel) to assess the kinetics of the photochemical cross-linking process (Figure 3a). The storage (G') and loss modulus (G'') of α-LAMA prehydrogels and α-LAMA hydrogels were dependent on both the mass ratio of MA to α-LA and the methacrylation degree

(Figure 3b). In general, both G' (storage modulus) and the gelation rate of α-LAMA exhibited an increase with a higher α-LAMA concentration and an elevated methacrylation degree.

At low methacrylation levels (24%) and/or low concentrations (10% w/v), α-LAMA solutions do not readily form hydrogels upon exposure to UV light (365 nm, 12 mW·cm^{-2}). Specifically, at a methacrylation degree of 24% for α-LAMA, the gelation times were 90 s for 30% (w/v) and 141 s for 25% w/v. However, with an increased methacrylation degree of 99%, for α-LAMA hydrogels at a concentration of 25% w/v and 30% w/v, the gelation times decreased to 15 and 20 s, respectively. It is obvious that the gelation time interval of α-LAMA solutions at stable concentrations decreases with an increasing degree of methacrylation. Compared with lower-
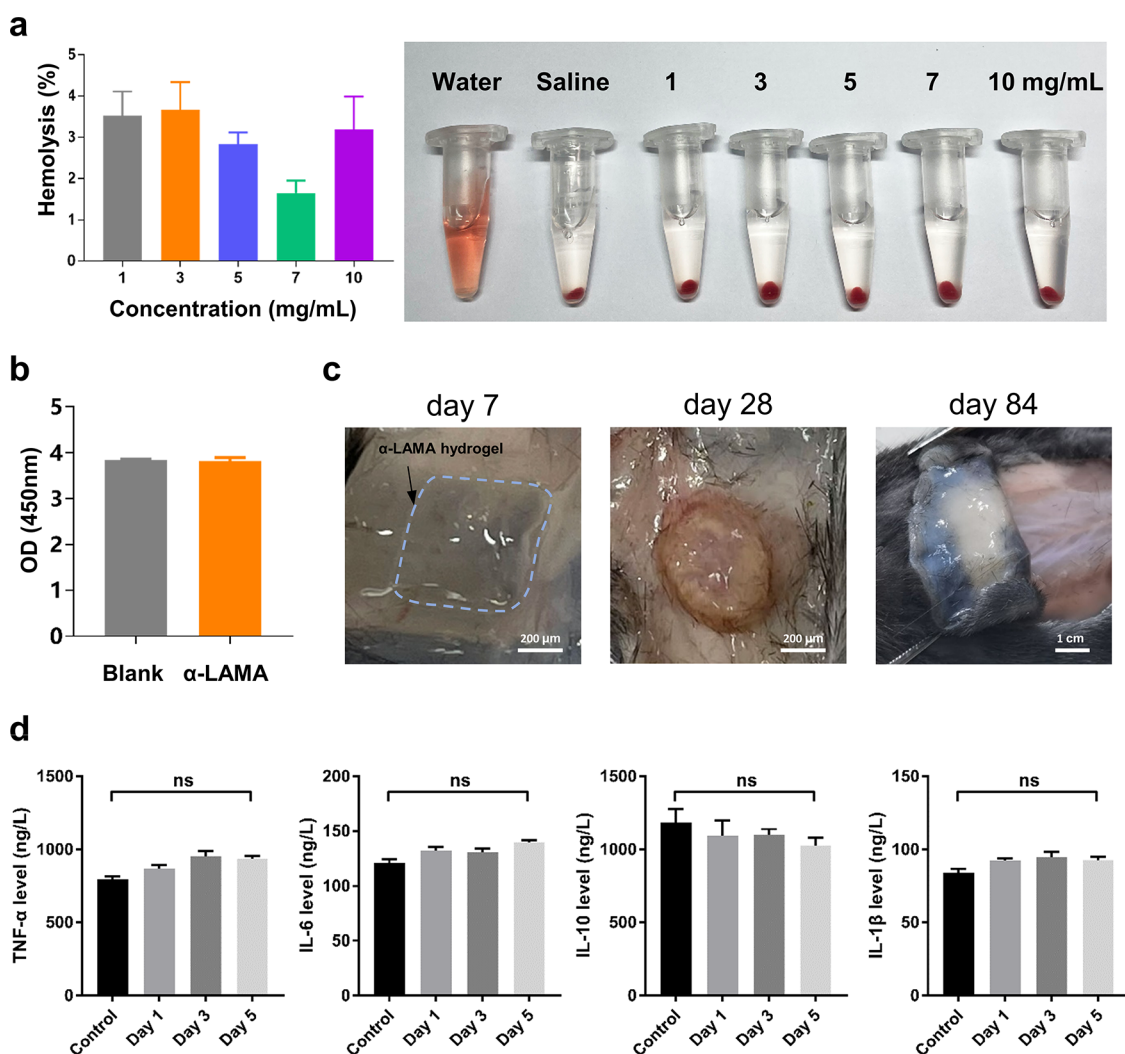
Figure 5. Biocompatibility evaluation of α-LAMA hydrogels. (a) Hemolysis of α-LAMA hydrogel extraction solution (1, 3, 5, 7, and 10 mg/mL) and photograph of the hemolysis test with water, saline, and α-LAMA hydrogel extraction solution (1, 3, 5, 7, and 10 mg/mL). (b) CCK8 test of the influence of α-LAMA hydrogels on cell activity. (c) Gross appearance images of α-LAMA hydrogels on day 7, day 28, and day 84 after implantation. (d) Concentrations of TNF-α, IL-6, IL-10, and IL-1β in control and implanted α-LAMA hydrogels.

concentration hydrogels, higher-concentration hydrogels were stiffer in addition to shorter gelation times.

After complete gelation, the final storage modulus for α-LAMA was 81.38 ± 0.61 (30% w/v), 68.33 ± 0.46 (25% w/v), 12.87 ± 0.43 (20% w/v), and 0.178 ± 0.01 kPa (15% w/v). The α-LAMA solutions (20% w/v) showed significantly faster gelation and a higher storage modulus than α-LAMA solutions with lower (15%) concentrations (P 0.0001) (Figure 3c). For biological applications such as the repair of internal wounds and tissue engineering, the swelling of hydrogels is most relevant (Figure 3d). After soaking the samples in PBS for 72 h, the swelling ratio was assessed at different time slots. The 15% α-LAMA hydrogel was found to have an increased volume and weight during the soaking phase, but the 20, 25, and 30% α-LAMA hydrogel showed no evident swelling. We suggest that the observed variation in osmotic pressure and molecular chain interlacing, together with α-LAMA concentration, may explain the observed change in the swelling ratio of the hydrogels.

α-LAMA hydrogels are light yellow in color when freshly formed due to the initiation stage of the cross-linking reaction caused the initiator (LAP) to break down, and free radical gave the hydrogels their yellow color. The hydrogels became translucent about 1 h after their formation, which may have been caused by LAP free radicals slowly being used up.

3.4. Different Preparation Modes of α-LAMA Hydrogels. Using scanning electron microscopy (SEM), the microstructures of several hydrogels were examined (Figure 4a); 20% α-LAMA hydrogels and 25% α-LAMA hydrogels showed dense pores, while 15% α-LAMA hydrogels had a loose porous structure. As the α-LAMA content increased, the pore size dropped; for example, the pore sizes of 15, 20, and 25% α-LAMA hydrogels were 68.8 ± 35.4, 32.5 ± 13.2, and 11.8 ± 8.3 μm, respectively. Presumably, a high-concentration polymer solution gives rise to a high-density network structure.

Apart from the bulk α-LAMA hydrogel, which is contingent upon the container's shape, the photo-cross-linkable α-LAMA is applicable to various processing techniques. The utilization of α-LAMA hydrogel microspheres is promising and realistic in the near future. The use of hydrogel microspheres has been widespread in tissue engineering,[20,21] drug administration,[22] gene sequencing,[23] and sensing applications.[24] In a microfluidic device, the α-LAMA solution could be emulsified into approximately 80 nm monodispersed microdroplets like it was

kept at the same concentration as the bulk solution. Upon UV irradiation and initiation with 0.05% w/v LAP, these microdroplets would give rise to hydrogel microspheres, akin to those formed in the bulk solution (Figure 4b,c). Through modifications to the oil and aqueous phase flow rates, the diameters of the microspheres could be customized. Further applications of future α-LAMA hydrogel microspheres are within reach. Additionally, a 1 mL syringe with a 26G needle was used to squeeze bulk α-LAMA hydrogel into an injectable paste (Figure 4d). By using a 6 W UV lamp for 45 s, the α-LAMA was chemically cross-linked into the α-LAMA hydrogel. The cross-linking density of the α-LAMA hydrogel was reduced by UV irradiation with less intensity and for a shorter period of time. The hydrogel fragmented as it was forced into the syringe and needle, greatly reducing the resistance to injection. On a digital light processing (DLP) 3D printing device, the potential of the α-LAMA solution as a bioink for 3D printing was assessed. The 20% (w/v) α-LAMA hydrogel precursor solution was successfully cross-linked into eagle designs with good shape integrity (Figure 4e). Important printing parameters such as printing speed, UV intensity, and solution temperature were comparable to those employed in well-linked bioinks such as GelMA. As a result, it is anticipated that the α-LAMA solution will be used as future bioinks and meet all the common DLP tools for the production of sophisticated, customized hydrogel scaffolds.

During the experiment, the free amino groups on α-LAs were methacrylated to create α-LAMA, which was then photo-cross-linked to create α-LAMA hydrogels while being exposed to an LAP photoinitiator. Photo-cross-linking employs visible or UV light for gelation at the original position under physiological pH conditions and at either room temperature or physiological temperatures. Photo-cross-linking has a number of benefits over conventional polymerization techniques, including the ability to influence the location and timing of the polymerization, quick curing times at physiological or room temperatures, and less escaping heat.[25] Injectable, highly adaptable hydrogels that can be photo-cross-linked may become the future desired products for biomedical applications. Compared to other injectable biopolymer-based hydrogels such as alginate hydrogels α-LAMA hydrogels have good biocompatibility and low immunogenicity.[26] Meanwhile, α-LAMA hydrogels have a relatively slower degradation rate in vivo and higher mechanical strength than most ECM hydrogels.[27] Previous experiments[28] used heat-induced gelation to create milk protein-based hydrogels,[29] which inhibited the incorporation of genetic material, living cells, and other heat-sensitive bioactive components.

3.5. Biocompatibility of α-LAMA Hydrogels.
Hemolysis testing is a useful method for assessing the hemocompatibility of biological materials. In general, materials with a hemolysis rate of less than 5% are considered to have good hemocompatibility, and lower hemolysis rates indicate better hemocompatibility.[30] In our present study, hemolysis tests were performed using different mass concentrations of α-LAMA hydrogel saline extracts (Figure 5a). The hemolysis rates of the α-LAMA hydrogel samples with different mass concentrations were less than 5%, which was below the assessment standard. The photographs of the hemolysis test showed that the positive control (pure water) group showed a red color with obvious hemolysis; the α-LAMA group was similar to the negative control (saline) group where no hemolysis was observed. The α-LAMA hydrogels are thus safe

and nontoxic to blood cells, even when the mass concentration of α-LAMA hydrogel was increased to 10 mg/mL. The cytotoxicity of α-LAMA hydrogel was examined by a CCK8 assay to demonstrate its suitability for biomedical applications (Figure 5b). In a CCK8 experiment, it was discovered that the α-LAMA hydrogel extract had comparable levels of cell viability to cells cultivated in DMEM, indicating that α-LAMA hydrogels have an overall high cell compatibility. Our results show that the newly synthesized α-LAMA hydrogels are safe, biocompatible, and biodegradable while meeting the basic criteria for biomaterials. Mice were subcutaneously implanted with a bulk α-LAMA hydrogel (Figure 5c). The bulk hydrogel was left unaltered for 7 days postimplantation. During this period, we observed signs of inflammation, as well as a mixed foreign-body reaction surrounding the hydrogel material. A dense capsule of mononuclear cells and deposited collagen was formed. The α-LAMA hydrogels dissolved totally 3 months after implantation, all the hydrogel materials were removed from the site of implantation without any remains, and α-LAMA hydrogel caused no signs of significant irritation during the experiment. Similar to animal tissues under physiological conditions, the skin and the associated organs in the hydrogel group, including the hair follicle, had a normal and healthy structure and morphology. At the sites of the skin implantation locations, hair started to grow back, demonstrating the safety of our α-LAMA hydrogel. Thus, it is feasible to predict how α-LAMA hydrogels will degrade in the future, with broader applications. Matrix metallopeptidase-9 (MMP-9) cleavage sites were discovered in α-LA,[31] supporting the subcutaneous breakdown of bulk hydrogels in mice. The α-LAMA hydrogel is flexible during processing, enabling it to take up various forms, including particles and bespoke scaffolds, and to allow for various other implantation techniques.

Additionally, animals implanted with α-LAMA hydrogels had their inflammatory cytokines measured in order to assess the biocompatibility of α-LAMA (Figure 5d). Using respective ELISA kits, the inflammatory cytokines TNF-α, IL-6, IL-10, and IL-1 were quantified on days 1, 3, and 5. The differences in all inflammatory markers between the implanted α-LAMA hydrogel group and the control group were negligibly small, indicating good in vivo biocompatibility of α-LAMA hydrogels.

3.6. Wound Healing Efficiency of α-LAMA Hydrogels.
According to the aforementioned experimental results, the α-LAMA hydrogel has adequate mechanical strength as well as good cytocompatibility. As a result, it can be utilized as a potent wound dressing to speed up healing. Photo-cross-linking is a promising technique for producing hydrogels as it can polymerize quickly at the site of the wound.[32] To assess the effectiveness of hydrogels in encouraging wound healing, a full-thickness cutaneous incision was performed experimentally in laboratory mice (C$_{57}$BL/6 N). For the in vivo testing, mice were allocated to three groups: the control group receiving no treatment; the Gauze group wrapped with gauze; and the α-LAMA group receiving treatment with α-LAMA hydrogels. We took images with a digital camera to track the wound-healing process (Figure 6a). On day 2, the injury in the control group was quite red, showing that the damaged area was inflamed. However, the α-LAMA group had very clean wounds throughout the treatment period compared with the Gauze and control groups. In addition, the wounds of mice treated with α-LAMA had accelerated closures on day 2, indicating a solid protective and anti-infective effect from the hydrogel (Figure 6b). By day 4, the α-LAMA group had decreased
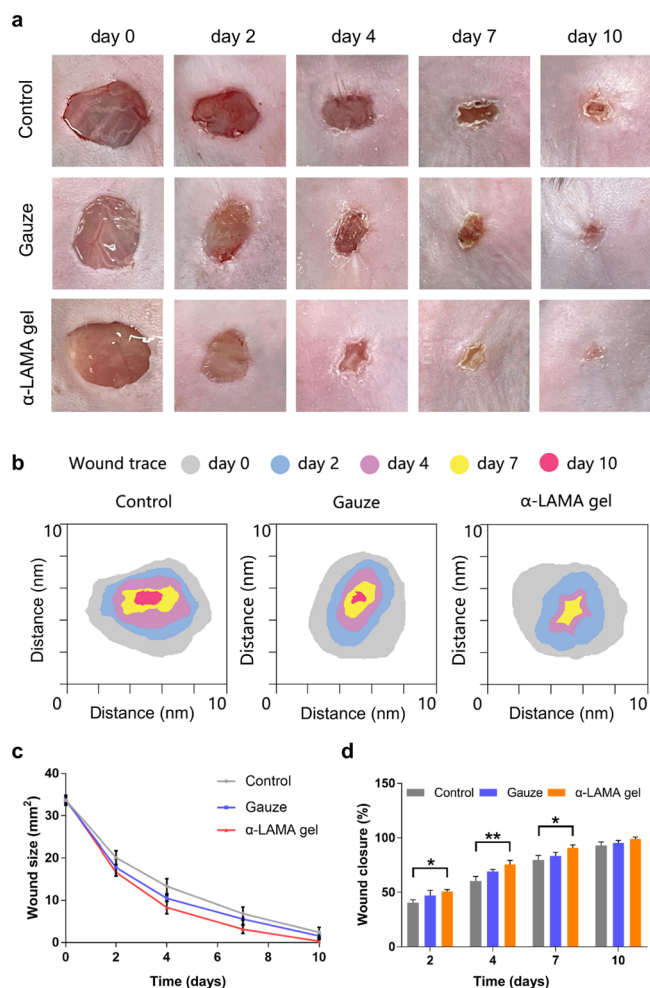
Figure 6. In vivo wound healing studies. (a) Representative pictures of wound tissues of different groups on days 0, 2, 4, 7, and 10. (b) Traces of wound-bed closure during 10 days for three groups. (c) Wound size over time in mice treated with different methods. (d) Wound closure for different groups during treatment.

Figure 7. Histopathological profiles of wounds in different groups. The overall and enlarged views of each group of slices are at the same scale. (a) Tissue slices stained with Hemotoxylin and eosin (H&E) from different groups on days 7 and 10. (b) Masson's trichrome stained wound tissue slices for different groups on days 7 and 10.

wound sizes from 33.9 ± 1.3 to 8.3 ± 1.7 mm^2, with a 75% wound closure (Figure 6c, d). With wound closures of 60 and 68% only, the animals from the control and Gauze groups still had wounds between 13.4 ± 2.2 and 10.5 ± 1.9 mm^2, respectively. Only wounds treated with α-LAMA were completely closed and covered with new epidermal tissue 10 days after the incision. Several wounds did not completely heal after receiving either no treatment or only gauze treatment. When compared with the control and Gauze groups, α-LAMA hydrogels demonstrated the most rapid wound contraction over the course of the 10-day period. This suggests that α-LAMA hydrogels improved and accelerated wound healing, which could be explained by the hydrogel properties that promote wound healing while acting as a physical barrier to stop bacteria from spreading over neighboring tissues.

Hematoxylin and eosin (H&E) staining and Masson trichrome staining were carried out to histologically assess the wound healing process (Figure 7a, b). On days 7 and 10, the control, Gauze, and α-LAMA group wound tissues underwent H&E staining. On day 7, large numbers of inflammatory cells were seen in the control and Gauze group, showing that inflammation was not under control. Both groups had few new epidermal tissues. However, by day 7, only
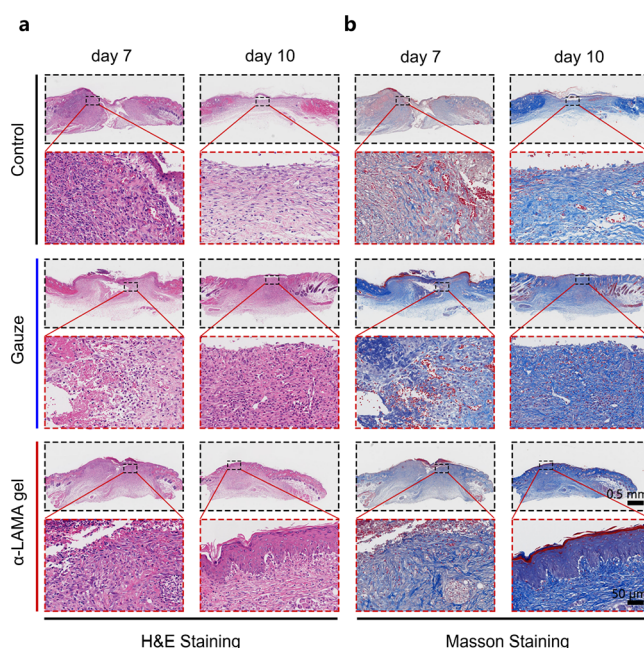
a few neutrophils were visible in the wound tissues of the α-LAMA group. Notably, new blood vessels and regenerated epidermis were seen, proving that α-LAMA hydrogel treatment accelerated the healing process. The complete healing of the damaged skin in the α-LAMA group after 10 days showed tissue regeneration. The control and Gauze groups, however, had numerous inflammatory cells and unhealing wound sites occasionally. The enhanced wound healing properties of the α-LAMA hydrogel were underlined by Masson's trichrome staining, revealing that more regenerated collagen was deposited in the wounds treated with α-LAMA hydrogel than in the other two groups. These results suggest that the α-LAMA hydrogel plays an important role in promoting wound healing.

4. CONCLUSIONS

Our study evaluated an α-LA-derived hydrogel as a wound dressing, which accelerates post-traumatic wound healing and promotes tissue regeneration. Bioactive peptides may have therapeutic properties that have not yet been fully explored or specifically addressed. Other materials in addition to hydrogels can be taken into consideration to increase the visibility of α-LA-derived biomaterials. As an example, sponges and nanoparticles based on α-LA could be used for tissue engineering and the delivery of medication.

α-LAs are frequently administered as dietary supplements, although their role in therapeutic settings has not been well explored. In this study, we presented α-LAMA hydrogels as a novel class of naturally protein-based biomaterials and discussed their potential applications as a material for medical tissue repair. Additionally, we established an economically and ecologically sustainable method for producing hydrogels based on milk protein on a larger, industrial scale.

■ AUTHOR INFORMATION

Corresponding Authors

Tanchen Ren − *Department of Cardiology, Cardiovascular Key Laboratory of Zhejiang Province, Second Affiliated Hospital, School of Medicine, Zhejiang University, Hangzhou 310027, China;* ● orcid.org/0000-0002-3382-7042; Email: rentanchen120@zju.edu.cn

Chengchen Guo − *School of Engineering, Westlake University, Hangzhou, Zhejiang 310023, China;* ● orcid.org/0000-0001-9253-3469; Email: guochengchen@westlake.edu.cn

Daxi Ren − *Institute of Dairy Science, College of Animal Sciences, Zhejiang University, Hangzhou 310027, China;* ● orcid.org/0000-0002-8016-0033; Email: dxren@zju.edu.cn

Authors

Yaqing Huang − *Institute of Dairy Science, College of Animal Sciences, Zhejiang University, Hangzhou 310027, China*

Qinchao Zhu − *Institute of Dairy Science, College of Animal Sciences, Zhejiang University, Hangzhou 310027, China*

Yang Zhu − *MOE Key Laboratory of Macromolecular Synthesis and Functionalization, Department of Polymer Science and Engineering, Zhejiang University, Hangzhou 310027, China*

Teresa G. Valencak − *Institute of Dairy Science, College of Animal Sciences, Zhejiang University, Hangzhou 310027, China;* ● orcid.org/0000-0002-7222-2265

Ying Han − *The State Key Laboratory of Fluid Power and Mechatronic Systems, School of Mechanical Engineering, Zhejiang University, Hangzhou 310027, China*

Complete contact information is available at:
https://pubs.acs.org/10.1021/acsomega.3c05793

Notes

The authors declare no competing financial interest.

■ REFERENCES

(1) Meyer, M. Processing of Collagen Based Biomaterials and the Resulting Materials Properties. *Biomed. Eng. Online* **2019**, *18*, 24.

(2) Janani, G.; Kumar, M.; Chouhan, D.; Moses, J. C.; Gangrade, A.; Bhattacharjee, S.; Mandal, B. B. Insight into Silk-Based Biomaterials: From Physicochemical Attributes to Recent Biomedical Applications. *ACS Appl. Bio Mater.* **2019**, *2*, 5460−5491.

(3) Bello, A. B.; Kim, D.; Kim, D.; Park, H.; Lee, S.-H. Engineering and Functionalization of Gelatin Biomaterials: From Cell Culture to Medical Applications. *Tissue Eng. B Rev.* **2020**, *26*, 164−180.

(4) Zhang, Y.; Hu, J.; Miao, Y.; Zhao, A.; Zhao, T.; Wu, D.; Liang, L.; Miikura, A.; Shiomi, K.; Kajiura, Z.; Nakagaki, M. Expression of Egfp-Spider Dragline Silk Fusion Protein in Bmn Cells and Larvae of Silkworm Showed the Solubility Is Primary Limit for Dragline Proteins Yield. *Mol. Biol. Rep* **2008**, *35*, 329−335.

(5) Jackson, J.; Janszen, D.; Lönnerdal, B.; Lien, E.; Pramuk, K.; Kuhlman, C. A multinational study of α-lactalbumin concentrations in human milk. *Nutr. Biochem.* **2004**, *15*, 517−521.

(6) Montagne, P.; Cuilliere, M. L.; Mole, C.; Bene, M. C.; Faure, G. Immunological and nutritional composition of human milk in relation to prematurity and mother's parity during the first 2 weeks of lactation. *Pediatric Gastroenterol. Nutr.* **1999**, *29*, 75−80.

(7) Kamau, S.; Cheison, S.; Chen, W.; Liu, X.; Lu, R. Alpha-lactalbumin: its Production Technologies and Bioactive Peptides. *Compr. Rev. Food Sci. Food Saf.* **2010**, *9* (2), 197−212.

(8) Sadiq, A.; Shah, A.; Jeschke, M. G.; Belo, C.; Qasim Hayat, M.; Murad, S.; Amini-Nik, S. The Role of Serotonin during Skin Healing in Post-thermal Injury. *Int. J. Mol. Sci.* **2018**, *19* (4), 1034.

(9) Sadiq, A.; Menchetti, I.; Shah, A.; Jeschke, M.; Belo, C.; Carlos-Alcalde, W.; Hayat, M.; Amini-Nik, S. 5-HT$_1$A Receptor Function Makes Wound Healing a Happier Process. *Front. Pharmacol.* **2018**, *9*, 1406−1406.

(10) Morr, C. V.; Ha, E. Y. Whey protein concentrates and isolates: processing and functional properties. *Crit Rev. Food Sci. Nutr.* **1993**, *33* (6), 431−476.

(11) Permyakov, E. A.; Berliner, L. J. alpha-Lactalbumin: structure and function. *FEBS Lett.* **2000**, *473* (3), 269−274.

(12) Farrell, H. M.; Jimenez-Flores, R.; Bleck, G. T.; Brown, E. M.; Butler, J. E.; Creamer, L. K.; Hicks, C. L.; Hollar, C. M.; Ng-Kwai-Hang, K. F.; Swaisgood, H. E. Nomenclature of the Proteins of Cows' Milk - Sixth Revision. *Dairy Sci.* **2004**, *87*, 1641−1674.

(13) Pellegrini, A.; Thomas, U.; Bramaz, N.; Hunziker, P.; von Fellenberg, R. Isolation and identification of three bactericidal domains in the bovine α-lactalbumin molecule. *Biochim. Biophys. Acta* **1999**, *1426*, 439−448.

(14) Guo, X.; Liu, Y.; Bera, Hriday; Zhang, H.; Chen, Y. α-Lactalbumin-Based Nanofiber Dressings Improve Burn Wound Healing and Reduce Scarring. *ACS Appl. Mater. Interfaces.* **2020**, *12* (41), 45702−45713.

(15) Liu, B.; Wang, R.; Li, Y. α-Lactalbumin Self-Assembled Nanoparticles with Various Morphologies, Stiffnesses, and Sizes as Pickering Stabilizers for Oil-in-Water Emulsions and Delivery of Curcumin. *J. Agric. Food Chem.* **2021**, *69* (8), 2485−2492.

(16) Ye, W. S.; Li, H. B.; Yu, K.; Xie, C. Q.; Wang, P.; Zheng, Y. T.; Zhang, P.; Xiu, J. F.; Yang, Y.; Zhang, F.; He, Y.; Gao, Q. 3d Printing of Gelatin Methacrylate-Based Nerve Guidance Conduits with Multiple Channels. *Mater. Des.* **2020**, *192*, No. 108757.

(17) Cheng, F. Y.; Su, C. H.; Yang, Y. S.; Yeh, C. S.; Tsai, C. Y.; Wu, C. L.; Wu, M. T.; Shieh, D. B. Characterization of aqueous dispersions of Fe(3)O(4) nanoparticles and their biomedical applications. *Biomaterials.* **2005**, *26* (7), 729−738.

(18) Yu, Y.; Tan, L.; Li, Z.; Liu, X.; Zheng, Y.; Feng, X.; Liang, Y.; Cui, Z.; Zhu, S.; Wu, S. Single-Atom Catalysis for Efficient Sonodynamic Therapy of Methicillin-Resistant Staphylococcus aureus-Infected Osteomyelitis. *ACS Nano* **2021**, *15* (6), 10628−10639.

(19) Cao, W. B.; Gao, C. Y. A Hydrogel Adhesive Fabricated from Poly(Ethylene Glycol) Diacrylate and Poly(Allylamine Hydrochloride) with Fast and Spontaneous Degradability and Anti-Bacterial Property. *Polymer.* **2020**, *186*, No. 122082.

(20) Li, F.; Truong, V. X.; Thissen, H.; Frith, J. E.; Forsythe, J. S. Microfluidic Encapsulation of Human Mesenchymal Stem Cells for Articular Cartilage Tissue Regeneration. *ACS Appl. Mater. Interfaces* **2017**, *9*, 8589−8601.

(21) Li, F.; Truong, V. X.; Fisch, P.; Levinson, C.; Glattauer, V.; Zenobi-Wong, M.; Thissen, H.; Forsythe, J. S.; Frith, J. E. Cartilage Tissue Formation through Assembly of Microgels Containing Mesenchymal Stem Cells. *Acta Biomater.* **2018**, *77*, 48−62.

(22) Lu, B.; Tarn, M. D.; Pamme, N.; Georgiou, T. K. Microfluidically Fabricated Ph-Responsive Anionic Amphiphilic Microgels for Drug Release. *J. Mater. Chem. B* **2016**, *4*, 3086−3093.

(23) Klein, A. M.; Mazutis, L.; Akartuna, I.; Tallapragada, N.; Veres, A.; Li, V.; Peshkin, L.; Weitz, D. A.; Kirschner, M. W. Droplet Barcoding for Single-Cell Transcriptomics Applied to Embryonic Stem Cells. *Cell.* **2015**, *161*, 1187−1201.

(24) Li, W.; Jiang, C.; Lu, S.; Wang, F.; Zhang, Z. J.; Wei, T. W.; Chen, Y. H.; Qiang, J.; Yu, Z. Y.; Chen, X. Q. A Hydrogel Microsphere-Based Sensor for Dual and Highly Selective Detection of Al^{3+} and Hg^{2+}. *Sens. Actuators, B* **2020**, *321*, No. 128490.

(25) Meng, W.; Gao, L.; Venkatesan, J. K.; Wang, G.; Madry, H.; Cucchiarini, M. Translational Applications of Photopolymerizable Hydrogels for Cartilage Repair. *Journal of experimental orthopaedics.* **2019**, *6*, 47.

(26) Taghipour, Y. D.; Hokmabad, V. R.; Bakhshayesh, Del; Asadi, N.; Salehi, R.; Nasrabadi, H. T. The Application of Hydrogels Based on Natural Polymers for Tissue Engineering. *Curr. Med. Chem.* **2020**, *27* (16), 2658−2680.

(27) Zhang, Y.; Xu, Y.; Gao, J. The engineering and application of extracellular matrix hydrogels: a review. *Biomater. Sci.* **2023**, *11*, 3784−3799.

(28) Choi, J. R.; Yong, K. W.; Choi, J. Y.; Cowie, A. C. Recent Advances in Photo-Crosslinkable Hydrogels for Biomedical Applications. *BioTechniques.* **2019**, *66*, 40−53.

(29) Muir, V. G.; Burdick, J. A. Chemically Modified Biopolymers for the Formation of Biomedical Hydrogels. *Chem. Rev.* **2021**, *121*, 10908−10949.

(30) Gorejová, R.; Oriňaková, R.; Macko, J.; Oriňak, A.; Kupková, M.; Hrubovčáková, M.; Džupon, M.; Sopčák, T.; Ševc, J.; Maskaľová, I.; Džunda, R. Electrochemical behavior, biocompatibility and mechanical performance of biodegradable iron with PEI coating. *J. Biomed. Mater. Res., Part A* **2022**, *110* (3), 659−671.

(31) Hu, Z.; Cao, W.; Shen, L.; Sun, Z.; Yu, K.; Zhu, Q.; Ren, T.; Zhang, L.; Zheng, H.; Gao, C.; He, Y.; Guo, C.; Zhu, Y.; Ren, D. Scalable Milk-Derived Whey Protein Hydrogel as an Implantable Biomaterial. *ACS Appl. Mater. Interfaces.* **2022**, *14* (25), 28501−28513. 29

(32) Kushibiki, T.; Mayumi, Y.; Nakayama, E.; Azuma, R.; Ojima, K.; Horiguchi, A.; Ishihara, M. Photocrosslinked gelatin hydrogel improves wound healing and skin flap survival by the sustained release of basic fibroblast growth factor. *Sci. Rep.* **2021**, *11* (1), 23094. 29